Theory for Metal Hydrides with Switchable Optical Properties

K. K. Ng[1,2], F. C. Zhang[1,3], V. I. Anisimov[4], and T. M. Rice[5]
[1] *Department of Physics, University of Cincinnati, Cincinnati, Ohio 45221*
[2] *Yukawa Institute for Theoretical Physics, Kyoto University, Kyoto 606-01, Japan*
[3] *Institute of Physics, Academia Sinica, Taipei, Taiwan*
[4] *Institute of Metal Physics, Russian Academy of Sciences, 620219, Ekaterinburg, GSP-170, Russia*
[5] *Theoretische Physik, ETH-Hönggerberg, 8093 Zürich, Switzerland*
(February 1, 2008)

Recently it has been discovered that lanthanum, yttrium, and other metal hydride films show dramatic changes in the optical properties at the metal-insulator transition. Such changes on a high energy scale suggest the electronic structure is best described by a local model based on negatively charged hydrogen (H^-) ions. We develop a many-body theory for the strong correlation in a H^- ion lattice. The metal hydride is described by a large U-limit of an Anderson lattice model. We use lanthanum hydride as a prototype of these compounds, and find LaH_3 is an insulator with a substantial gap consistent with experiments. It may be viewed either as a Kondo insulator or a band insulator due to strong electron correlation. A H vacancy state in LaH_3 is found to be highly localized due to the strong bonding between the electron orbitals of hydrogen and metal atoms. Unlike the impurity states in the usual semiconductors, there is only weak internal optical transitions within the vacancy. The metal-insulator transition takes place in a band of these vacancy states.
PACS numbers: 71.30.+h, 71.15.Mb, 71.55.Ht, 72.15.Eb

I. INTRODUCTION

Huiberts *et al.* [1] have recently reported dramatic changes in the optical properties of lanthanum, yttrium, and other rare earth hydride films [2] with changing hydrogen content. This phenomenon has also been recently observed in other metal hydrides, such as Gd-Mg alloy hydrides [3]. By changing the hydrogen gas pressure, or by electrochemical means [5] the films can be continuously and reversibly switched from a shiny mirror (good metal) to a transparent window (insulator) in a fraction of a second. Although many metal-insulator transitions are known, this type of switchable optical phenomena is very unusual, and potentially of considerable technological importance since the transition leads to spectacular effects in the *visible* light region. For example, this class of materials is very different from the previously reported charge density wave compound $KMoO_3$. In that compound, the frequency dependent conductivity may be changed by replacing some of Mo atoms by W [4], but the change in reflectivity is in the infrared or lower frequency region, while the metal hydrides show dramatic changes in the visible. Since the hydrides are easily tunable, this class of compounds is also ideal for basic research to understand the metal-insulator transition in general. Furthermore, since the optical switching is realized at room temperature and at normal pressure, and since there appears to be considerable scope for shortening the time-scale of the transition through chemical or electrochemical means [6], the phenomenon is very attractive for optical devices.

As Huiberts *et al.* [1] reported, the transitions measured in the optical transmission and in the electric resistivity appear at the same hydrogen concentration $x = x_c \simeq 2.80$ for both the YH_x and LaH_x. The optical gap in the insulating phase is ~ 1.8 eV for LaH_3 and ~ 2.8 eV for YH_3. The transition is clearly of electronic origin in the lanthanum hydrides where the crystal structure remains face centered cubic (fcc) for $2 \leq x \leq 3$. In the yttrium hydrides, there is evidence that the observed metal-insulator transition is also of electronic origin [6].

The electronic structure underlying this behavior was poorly understood − indeed the standard local density approximation (LDA) calculations failed to predict a metal-insulator transition at all. In 1970, Switendick [12] used a non-self-consistent approximation to calculate the electronic structure of the YH_3, and found an energy gap of 1.5 eV. But more sophisticated state-of-the-art self-consistent LDA calculations by Dekker *et al.* [13], Wang and Chou [14] predict that LaH_3 and YH_3 are metals or semimetals.

The structure changes are especially small in the LaH_x films, which may be considered as a prototype for this class of compounds. The La atoms always form a fcc lattice with two H atoms occupying tetrahedrally coordinated sites. As x changes from 2 to 3, the octahedrally coordinated sites go from empty to fully occupied and a good metal evolves to a transparent insulator. The crystal structure is shown in Fig. 1. The actual lattice constants of the dihydride and the trihydride are 10.7051 a.u. (1 a.u.= 0.528 Å) and 10.5946 a.u. respectively. The slight contraction due to the addition of H atom in LaH_3 indicates strong hybridization between La and H atoms. But the small difference in lattice constant is insignificant, and will be neglected in our further consideration.

In the metal hydrides, the hydrogen atom attracts one more electron and forms a negative hydrogen ion H^-.

The rare earth metal such as La has a formal valence 3+. In a dihydride such as LaH_2, the 1s-orbital of the hydrogen bands (H bands) are filled, leaving 1 electron per unit cell in the La conduction bands. This gives metallic behavior. In a trihydride such as LaH_3, the H bands can hold all six valence electrons per unit cell. However, in the LDA calculations there is an overlap between the H and La 5d-orbital bands, leading to a metal or semimetal rather than the observed transparent insulator. The H^- ion is a difficult case for the LDA, and a careful treatment of the correlation between the two electrons is required in order to obtain the bound H^- ion state with binding energy of 0.7 eV (see next section). The poor treatment of correlations is most likely the reason why LDA is unable to explain the transparent insulating behavior of LaH_3. It is well known that the LDA underestimates the energy gap in semiconductors. This problem seems much more pronounced in rare earth hydrides: LDA predicts a metallic state for an insulator with substantial gap.

There has been considerable theoretical activity since the original discovery [16,17,14,19,20]. In an early Letter [16], we examined the role of electron correlation and proposed a local model to describe the electronic structure and the metal-insulator transition in these hydrides. The purpose of the present paper is to refine our calculations and to present a more complete theory for these hydrides. Recently, Eder *et al.* [17] have proposed a theory based on the occupation-dependent hoppings on H sites and examined a Kondo-like-insulator model for YH_3. Their theory has much in common with ours. Very recently Chang *et al.* [20] reported GW method calculations for LaH_3 and found a gap of ~ 0.5 eV. This again indicates the importance of electron correlation. On the other hand, Kelly *et al.* [19] proposed that the insulating nature of YH_3 may be explained within the LDA due to a more complicated hexagonal structure for Y. Their proposal, however, has difficulty explaining the insulating nature of many other hydrides, such as La hydrides, whose crystal structure is a always simple fcc.

In this paper, we examine the importance of electron correlation in metal hydrides, and develop a many-body theoretic framework to study their electronic structure. LaH_3 may be viewed as a Kondo insulator [16,17] if we start with metallic phase LaH_2 and consider every additional H atom to a be Kondo impurity. LaH_3 may also be viewed as a band insulator due to the strong electron correlation, which suppresses the overlaps between the H and metal bands. When the H concentration is reduced in the LaH_3 structure, the elementary entities are the H-vacancies. We find highly localized electronic states centered on these vacancies. The metal-insulator transition takes place in a band of these vacancy states. The paper is organized as follows.

In section II, we first review an appropriate wavefunction for a single H^- ion in free space incorporating the electron correlation explicitly. We then extend the discussion to a lattice of H^- ions, and use a microscopic model to calculate the electron motion (or the effective hopping integrals) in such a lattice.

In section III, we propose that the metal hydrides are best described by a large U-limit Anderson lattice Hamiltonian, with U the electron Coulomb repulsion on the H atom. At every H site, electron state is either singly or doubly occupied. The electron hopping integrals between H sites are described by those obtained in our microscopic calculations in section II. Other parameters are extracted from the LDA calculations. We use the Gutzwiller method to study this model Hamiltonian for the hydrides within this method the local constraint on the H sites is replaced by a set of renormalization factors.

In section IV we present our results for the electronic structure of LaH_2 and LaH_3. The former is found to be a metal, and the latter an insulator, in agreement with experiments.

Section V consists of the study of the localized H vacancy state in LaH_3 and the H impurity state in LaH_2. The localized vacancy state is proposed to be the elementary entity in the hydrides and to be responsible for the metal-insulator transition. We will use finite size calculations to verify the symmetry and localized nature of the vacancy states. In section VI we use the calculated electronic band structure to study the optical conductivity and density of states. We perform finite size calculations and compare the results to experimental data.

II. ELECTRON CORRELATION IN NEGATIVELY CHARGE HYDROGEN IONS

In this section we start by reviewing the electron correlation in a single negatively charged hydrogen ion (H^- ion) and the importance of the cooperative motion of the two electrons around the proton. We will then describe a local model for studying the many-body problem of a lattice of H^- ions. A microscopic model calculation will be presented to estimate the effective kinetic energy for the electrons in a H^- ion lattice.

A. A single H^- ion in free space

This is a venerable but interesting problem [21–25]. It was carefully studied by astrophysicists back in the 1950's, when the H^- ion was found to be of great importance for the opacity of the atmosphere of the sun and similar stars. Since hydrogen contains only one proton, the smallest charge of all nuclei, the Coulomb attraction between an electron and its nucleus is the weakest and when an additional electron is added to a neutral H atom, the Coulomb repulsion between the two electrons becomes crucially important. Electron-electron correlation has the largest effect in H atoms compared to other atoms. As found by Chandrasakhar [22], Bethe and Salpeter [21], and Hylleraas *et al.* [23], a careful treatment of the correlation between the two electrons is nec-

essary to obtain the correct binding energy of about 0.7 eV. This shows that the H^- ion is a bound state due to a strong electron correlation effect.

Variational trial wavefunctions have been applied to the H^- ion for there is no exact analytic solution for the ion. Wavefunctions with up to 24 variation parameters [23] were proposed to give the best estimate of the binding energy. On the other hand, there is a simple but excellent trial wavefunction introduced by Chandrasakhar in the 1940's [22] to describe the electron correlation in H^-.

$$\psi(1,2) = (e^{-ar_1-br_2} + e^{-ar_2-br_1})(1 + c|\mathbf{r}_1 - \mathbf{r}_2|)\chi, \quad (1)$$

where $(\mathbf{r}_1, \mathbf{r}_2)$ are the electron coordinates with respect to the proton, χ is the spin singlet spinor, and the constants $a = 1.075$, $b = 0.478$, $c = 0.312$ in atomic units. As illustrated in Fig. 2, the wavefunction can roughly be visualized as an inner electron of radius ~ 1, and an outer electron of radius ~ 2 orbiting around the proton. The electron correlation is described by the term $c|\mathbf{r}_1 - \mathbf{r}_2|$, which tends to keep the two electrons apart. This is similar to the Laughlin's wavefunctions for the fractional quantum Hall states, where electrons in high magnetic fields tend to stay apart and form a quantum liquid [26]. One should notice that the second electron does not reside in the same orbital as the first electron although they have opposite spins, nor does it occupy the $2s$ orbital which has a very different radial wavefunction. In this wavefunction the electrons are in a spin singlet state while the spin triplet state is unbound. The wavefunction of Eq. (1) gives a ground state energy of H^- ion very close to the best estimate of Hylleraas [23] using 24 variational parameters. Note that the choice of the form of the variational wavefunction is very subtle and other simple choices mostly give an unbound electron. The standard LDA calculations for a single H^- do not give a bound state [27].

The simple wavefunction of Eq. (1) will be used to develop a many body theory for the H^- ion lattice. The more refined 24 parameters wavefunction may produce a better result, but the calculation of hopping integrals involving such a complicated wavefunction will be very difficult and time consuming.

B. H^- ions in crystal

Since a single H^- ion is a bound state, the ionic picture should be valid in certain hydride crystals. A local description is suggested by the recently observed insulating gap in LaH_3 and YH_3. This led us to examine the effect of correlations on the H^- band width. In this section we shall focus on H^- ions. The effect of rare earth ions through their hybridization with H^- ions is also significant, and will be discussed in a later section. The form of the H^- bands in a many body theory is determined by the spectrum of the states obtained by removing an electron from a lattice of H^- ions. We will use a local model, namely an orthogonal tight-binding model to describe the hole motion. Then the energy spectrum is determined by the effective hopping integrals $t(d)$ of an electron from a H^- ion to a neutral H atom at distance d. Below we shall estimate $t(d)$ from a microscopic model, in which the correlated Chandrasakhar wavefunction Eq. (1) will be employed.

We consider a single pair consisting of one H^- ion and one H atom separated by a distance d as illustrated in Fig. 3. This results in a H_2^- ion, an ion with three electrons moving around two protons. Previous studies have shown that H_2^- ion is a bound negative ion [24] for $d > 3$ a.u., the range of interest here (the nearest H-H distance separation in LaH_3 is 4.58 a.u.). For $d < 3$ a.u., H_2^- ion becomes unstable and dissociates into H_2 and an unbound, free electron. When a H^- ion and H atom are brought together from infinity, the ground state manifold of H_2^- splits into odd$(-)$ and even$(+)$ parity states with respect to the center of mass of the two protons. It is this splitting that determines the effective hopping matrix element $t(d)$. Let E_- and E_+ be the energies of the odd and even parity states respectively, then we have

$$t(d) = (E_- - E_+)/2. \quad (2)$$

This relation may be understood as follows. Consider an electron which hops between two atoms of the same atomic energy with hopping integral t. Then, the energy of the even parity state is t and the energy of the odd parity state is $-t$, the energy difference between the two states is $(E_+ - E_-) = 2t$. In the H_2^- ion problem, the singlet spin gives an additional sign change, as does Eq. (2).

The H_2^- ion is a three-body problem and therefore no exact analytic solution is available. Yet a suitable approximation can still give a reasonably good ground state energy. We construct the lowest energy states of different parities using the single site states of H^- ion, Eq. (1), and the neutral H-atom. Let $\phi(\alpha)$ be the hydrogen ground state wavefunction (the Bohr atom solution) of the αth electron (Fig. 3). Then the three electron states of the H_2^- with odd$(-)$ and even$(+)$ parities are given by:

$$\Psi_\pm = \Phi_{i,j} \pm \Phi_{j,i}, \quad (3)$$

where

$$\Phi_{i,j} = A[\psi_i(1,2)\phi_j(3)]. \quad (4)$$

A is the antisymmetric operator to assure the antisymmetry of the wavefunction $\Phi_{i,j}$ when two electrons are interchanged. The corresponding energies of $\Psi_\pm$ are given by

$$E_\pm = \frac{\langle\Psi_\pm|h|\Psi_\pm\rangle}{\langle\Psi_\pm|\Psi_\pm\rangle} = \frac{\langle\Phi_{i,j}|h|\Phi_{i,j}\rangle \pm \langle\Phi_{j,i}|h|\Phi_{i,j}\rangle}{\langle\Phi_{i,j}|\Phi_{i,j}\rangle \pm \langle\Phi_{j,i}|\Phi_{i,j}\rangle}, \quad (5)$$

where h is the Hamiltonian for the H_2^- system,

$$h = \sum_{\alpha=1}^{3}(\frac{p_\alpha^2}{2m} - \frac{e^2}{r_\alpha} - \frac{e^2}{r'_\alpha}) + \sum_{\alpha<\beta}^{3}\frac{e^2}{r_{\alpha\beta}}. \quad (6)$$

In Eq. (6), $p_\alpha^2/2m$ is the kinetic energy, r_α and r'_α are the distances of the αth electron to the two protons respectively, and $r_{\alpha\beta} = |\mathbf{r}_\alpha - \mathbf{r}_\beta|$. It is convenient to split h into two parts, $h = h_0 + h'$, with h_0 the Hamiltonian without the interaction between the sites i and j,

$$h_0 = \sum_{\alpha=1}^{3}(\frac{p_\alpha^2}{2m}) - \frac{e^2}{r_1} - \frac{e^2}{r_2} - \frac{e^2}{r'_3}. \quad (7)$$

h_0 approaches to h at the limit of large inter-proton distance. h' describes the interaction energy between the H^--ion and the H atom.

Substituting $\Phi_{i,j}$ into Eq. (5) in terms of ϕ_i and ϕ_j, we find the two numerator terms to be the following combinations of integrals of h_0 and h',

$$\langle\Phi_{i,j}|h|\Phi_{i,j}\rangle = 3(E_0 + E_1) - 3(E_0 a_2 + b_2), \quad (8)$$
$$\langle\Phi_{j,i}|h|\Phi_{i,j}\rangle = 3(E_0 a_3 + b_3) - 3(E_0 a_1 + b_1), \quad (9)$$

where $E's$ and $a's$ are defined as,

$$\begin{aligned} E_0 &= \langle(12)_i 3_j|h_0|(12)_i 3_j\rangle, & E_1 &= \langle(12)_i 3_j|h'|(12)_i 3_j\rangle, \\ a_1 &= \langle(12)_i 3_j|1_i(23)_j\rangle, & b_1 &= \langle(12)_i 3_j|h'|1_i(23)_j\rangle, \\ a_2 &= \langle(12)_i 3_j|(23)_i 1_j\rangle, & b_2 &= \langle(12)_i 3_j|h'|(23)_i 1_j\rangle, \\ a_3 &= \langle(12)_i 3_j|3_i(12)_j\rangle, & b_3 &= \langle(12)_i 3_j|h'|3_i(12)_j\rangle. \end{aligned} \quad (10)$$

For simplicity, we define $|(12)_i 3_j\rangle \equiv |\psi_i(1,2)\phi_j(3)\rangle$. Note that E_0 is simply the sum of the energies of the independent H^- ion and H-atom. Eq. (5) now becomes,

$$E_\pm = E_0 + \frac{E_1 - b_2 \pm (b_3 - b_1)}{(1 - a_2) \pm (a_3 - a_1)}. \quad (11)$$

These integrals are calculated numerically for a few values of the inter-proton distance d and are listed in Table I.

For H_2^- ion, the ground state is of odd parity. The energy of H_2^- ion we obtained in the present approach compares favorably with the best estimates reported previously using different methods [24,25]. In Fig. 4, we plot our values of E_- as a function of inter-proton distance d. Fischer-Hjalmars [25] used a similar approach, but ignored the correlation term in the Chandrasakhar wavefunction probably due to the limited computational power in the 60's. Our energies are much lower than theirs. This indicates that the electron correlation has a significant contribution to the ground state energy of the H_2^- ion. It comes as a surprise that our result is even somehow better than that of Taylor and Harris for $d > 4$ a.u.. Taylor and Harris [24] used a rather complicated wavefunction which involves many linear and nonlinear variational parameters. Their parameters are distance dependent and variational procedures were carried out for each of d. The comparison with their result indicates that the Chandrasakhar wavefunction that we used is very successful on capturing the most essential physics in a single H_2^- ion. This also justifies our estimate for the electron hopping integrals in the H^- ion lattice. The present calculations give a higher ground state energy for $d < 4$ a.u. than that of Taylor and Harris. This is understandable. For smaller distances d, our method constructing a wavefunction based on individual H^- and H orbitals becomes poor. However, the distance between hydrogen ions in lanthanum hydrides is always greater than 4 a.u., the region of our interest. Therefore we are confident in our estimate of the hopping integral.

Using Eqs. (2) and (11), we find that the hydrogen hopping integral t can be written in terms of the integrals in Eq. (10) as,

$$t = -\frac{(E_1 - b_2)(a_1 - a_3) - (b_1 - b_3)(1 - a_2)}{(1 - a_2)^2 - (a_1 - a_3)^2}, \quad (12)$$

giving values for the hopping integral between the neighboring H_{tet} and H_{oct} (see Fig. 1), $t_2 = -0.748$ eV ($d = 4.58$ a.u.), and between the two nearest H_{tet} atoms, $t_1 = -0.523$ eV ($d = 5.29$ a.u.).

In the above calculations, we focus on the H_2^- ion, and have neglected the Madelung potential of other H^- ions and metal ions in the lattice. These ions create an electric field on the H_2^- ion under consideration, which reduces the amplitudes of hopping integrals. This effect is often called a crystal field effect, and will be discussed next.

C. Crystal field effect

In the above estimation for the hopping integrals, we have neglected the La^{3+} ions as well as surrounding H^- ions. In an ionic picture, the La^{3+} and H^- ions generate a crystal field at each H site. Therefore the Hamiltonian in Eq. (6) should be modified to include the Coulomb interactions between the electrons in the H_2^- ion under consideration and all other H^- ions and La^{3+}. We will treat the crystal field effect as a perturbation, whose Hamiltonian is given by

$$h'' = \sum_{\mathbf{R}} -\frac{Z(\mathbf{R})e^2}{|\mathbf{r}_2 - \mathbf{R}|}, \quad (13)$$

where the sum runs over the La^{3+}, and all other H^- ions. $Z(\mathbf{R})e$ represents the charge of an ion located at $\mathbf{R}$ ($Z(\mathbf{R}) = 3$ for La^{3+} ion, and $Z(\mathbf{R}) = -1$ for H^- ion). Then the first order correction to the energies $E_\pm$ is given by

$$\delta E_\pm = \frac{E'_1 \mp b'_1}{1 \mp a_1}, \quad (14)$$

with

$$E'_1 = \langle(12)_i 3_j|h''|(12)_i 3_j\rangle, \quad b'_1 = \langle(12)_i 3_j|h''|1_i(23)_j\rangle. \quad (15)$$

Accordingly, the change of the hopping integral, $\delta t = (\delta E_- - \delta E_+)/2$ is found to be

$$\delta t = -\frac{E_1' a_1 - b_1'}{1 - a_1^2}. \tag{16}$$

In the calculation of δt, we shall use a summation technique similar to the usual calculation of the Madelung constant to keep the charge neutrality of the summed ions. For a reason to be explained later, we consider δt_1, the change of the hopping integral between the nearest neighbor (n.n.) tetrahedral hydrogens. We consider the midpoint of the H_2^- in question as the origin (Fig. (6)), and calculate δt_1 from the contributions of all the other ions within a cubic cell centered at the origin. As the size of the cubic cell increases, δt_1 changes monotonically and saturate. In Table II, we list δt_1 as the size of the cubic cell increases. δt_1 starts to converge for a $4 \times 4 \times 4 a_0^3$ cubic cell and reaches a value $\delta t_1 = 0.230$ eV at $6 \times 6 \times 6 a_0^3$ (See Table II).

Note that t_1 is negative , and δt_1 is positive. The crystal field reduces the magnitude of the hopping integral. This is consistent with our intuition. The net effect of surrounding ions is from positive charged ions, because of the charge neutrality (H_2^- has a net charge of $-e$). The positive charged ions (La^{3+}) attract the outer electron of a H^- ion, and reduce its hopping amplitude to a neighboring hydrogen.

We thus estimate the hopping integral in the presence of the crystal field, to be $\tilde{t}_1 = -0.293$ eV. This is about 60% of the value without the crystal field. We see that the crystal field significantly reduces the hopping integral. However, the estimate for t_2 is more complicated because of the asymmetry of the crystal with respect to the tetrahedral and octahedral hydrogen atoms. Assuming the same percentage reduction for t_2, we estimate $\tilde{t}_2 = -0.419$ eV. Note that our estimate is based on an ideal ionic approach within which screening effects are neglected, so that the actual reduction of the t's is expected to smaller.

III. MICROSCOPIC MODEL FOR METAL HYDRIDES

A. Model Hamiltonian

Having a better understanding of the electron correlation in H^- and its effect on the electron hopping matrix between the H^- ions, we are ready to proceed to an appropriate microscopic model for the rare earth hydrides. We introduce a large U-limit Anderson lattice Hamiltonian to model the system. In the tight binding representation, the Hamiltonian, in the second quantization language, is given by:

$$H = H_h + H_{La} + H_{mix}, \tag{17}$$

where the three terms represent the hydrogen, the lanthanum, and their hybridization respectively. The hydrogen part is

$$H_h = \sum_{i,s} \epsilon_i^h h_{i,s}^\dagger h_{i,s} + \sum_{\langle i,j \rangle} t_{i,j}^h \left(h_{i,s}^\dagger h_{j,s} + \text{h.c.} \right), \tag{18}$$

where i sums over all the occupied H atoms, and $\langle i,j \rangle$ neighboring pairs. $h_{i,s}$ is the destruction operator for an electron of spin s on the H site i. There is a constraint for electrons on each H site i,

$$\sum_s h_{i,s}^\dagger h_{i,s} \geq 1. \tag{19}$$

Eq.(19) is to exclude the empty electron state at any hydrogen site. We will discuss this point further below. In Eq.(18), ϵ_i^h is the atomic energy of the outer electron at site i, which is -0.7 eV in free space and will be modified in crystal. $\epsilon_i^h = \epsilon_t$ at the tetrahedral site, and $\epsilon_i^h = \epsilon_o$ at the octahedral site. t_{ij}^h are the hopping integrals between two H sites as estimated in section II B. The lanthanum part of the Hamiltonian is given by

$$H_{La} = \sum_{i,\alpha,s} \epsilon_\alpha^{La} d_{i,\alpha,s}^\dagger d_{i,\alpha,s} + \sum_{\substack{\langle i,j \rangle \\ \alpha,\beta,s}} t_{i,j}^{\alpha,\beta} \left(d_{i,\alpha,s}^\dagger d_{j,\beta,s} + \text{h.c.} \right), \tag{20}$$

where $d_{i,\alpha,s}$ destroys an electron of orbital α and spin s on the La-site i. We shall only include the five La-5d orbitals labeled by α. They are closest to the chemical potential and therefore most relevant.

The La-6s orbital will be neglected since its energy levels are high above the fermi energy. ϵ_α^{La} denotes the atomic energy of orbital α at the the La-site. $t_{i,j}^{\alpha,\beta}$ is the hopping integral between orbital α at site i and orbital β at site j.

H_{mix} describes the electron hybridization between H and La sites,

$$H_{mix} = \sum_{i,j,\alpha,s} V_{i,\alpha,j} \left(d_{i,\alpha,s}^\dagger h_{j,s} + \text{h.c.} \right), \tag{21}$$

where $V_{i,\alpha,j}$ is the hopping integral between La site i of orbital α and H-site j.

We now discuss on the physical meaning of the constraint Eq. (19). As we examined in the previous section, the two electrons in the H^- ion are very different in energy. The outer electron has a binding energy 0.7 eV, while the binding energy for the inner one is 13.6 eV in free space. At low energies, the inner electron is always occupied, and only the outer electron is mobile. The constraint (19) is a mathematical description of this physics. If we define a H^- ion as a vacuum, namely a fully filled 1s shell, then a neutral H atom is a single-hole state, and H^+ is a double-hole state. The constraint Eq. (19) prohibits a doubly occupied hole configuration at any H

site. Our model (17) is a large U-limit Anderson lattice model, where U is the Coulomb repulsion between two holes on the same H site.

The important difference between inner and outer electrons in hydrides was also discussed by Eder *et al.* [17]. These authors describe hydrogen as a breathing atom, whose radius is much larger for H^- than for H. Eder *et al.* proposed an Anderson lattice model, where the hopping integrals depend on electron occupation number on the H site. They carried out an impurity-like calculation to examine the stability of the Kondo-like singlet configuration similar to that proposed in our earlier work [16].

We now apply Eq. (17) to LaH_x. In LaH_x the lanthanum sites are always fully occupied while the occupation of hydrogen sites depends on x. The properties of Hamiltonian (17)-(21) also depends on the parameter values. The effective hopping integrals $t^h_{i,j}$ between two H sites have been estimated in section II B. The other parameters may be extracted from the local density approximation calculations, which will be described in the next section.

The Hamiltonian (17) with the local constraint is a many-body problem. We will solve the model for different values of the H concentration x using the Gutzwiller method [28,29], which has been well established in study of heavy electron and mixed valence compounds.

B. Parameters fitting from LDA calculations

The LDA does not treat the electron correlation properly. However we expect the LDA to give reasonably good estimates for other parameters in the hydrides. We carried out LDA calculations for LaH_3, used a tight binding model to fit to the LDA results and extracted parameters for model (17). For simplicity, we consider only hopping integrals between the nearest neighbor (n.n.) tetrahedral H-sites (t_2), between the neighboring H_{tet} and H_{oct} sites (t_1), between the n.n. H and La sites, and between the n.n. and the next n.n. La sites. Since the lattice constant changes insignificantly for $3 \leq x \leq 2$ in LaH_x, we shall assume the parameters remain unchanged.

In Fig. 7 we show our LDA results for the band structure of LaH_3 and LaH_2. Other LDA calculations gave similar results [13,14]. We use a tight binding model, identical to Eq. (17) but with no constraint Eq. (19), to fit Fig. 7(a) for LaH_3. The fitted band structure is plotted in Fig. 8(a), and the fitting parameters are listed in Table III. In the fitting, we pay most attention to those states near the chemical potential. The same set of parameters fit the LDA bands of LaH_2 as well, see Fig. 7(b) and Fig. 8(b).

Since all s-s, s-d and d-d orbital bondings can be expressed as a linear combinations of σ-bonds (angular momentum along the bonding axis $m = 0$), π-bonds ($m = 1$) and δ-bonds ($m = 2$), the hopping integrals $t^h_{i,j}$, $t^{\alpha,\beta}_{i,j}$ and $V_{i,\alpha,j}$ can be represented by a few bonding integrals. They are given by

$$\begin{aligned} t^h_{i,j} &= V^{h-h}_{ss\sigma}, \\ t^{\alpha,\beta}_{i,j} &= a_{\alpha,\beta}(l,m,n)V^{La-h}_{sd\sigma}, \\ V_{i,\alpha,j} &= b^{(1)}_\alpha(l,m,n)V_{dd\sigma} + b^{(2)}_\alpha(l,m,n)V_{dd\pi}. \end{aligned} \tag{22}$$

where $V^{h-h}_{ss\sigma}$ ($V^{La-h}_{sd\sigma}$) is σ-bonding integrals between H $1s$ and H $1s$ (La $5d$) orbitals, while $V_{dd\sigma}$ and $V_{dd\pi}$ are σ- and π-bonding integrals of La $5d$ to $5d$ orbitals, respectively. The contribution from δ-bonding is generally small and is ignored. The coefficients $a_{\alpha,\beta}$ and b_α's are functions of the direction cosines (l,m,n) from site i to site j. These coefficients have been derived by Slater and Koster [30] based on the symmetry. The number of fitting parameters is now reduced since there are only a few bonding integrals. It is worth to note that the H hopping integrals obtained from LDA, $V^{o-t}_{ss\sigma} = -0.79$ and $V^{t-t}_{ss\sigma} = -0.4$, are larger than that calculated from the local model, $\tilde{t_2} = -.419$ and $\tilde{t_1} = -0.293$. It justifies that the electron correlation plays an important role in the H hopping integrals. Therefore, we will use $\tilde{t_1}$ and $\tilde{t_2}$ for the H hopping integrals in the future calculations.

Although there are some discrepancies with the LDA band structure for high energy La bands, the main concern here should be the position of the lowest La bands and the highest H bands which are responsible for both the transport and optical properties. Bear in mind that our motivation is to reproduce the essential qualitative features rather than a very accurate description and hence the fitting may not be unique. We have carried out the same fitting procedures for Dekker's LDA band calculation [13]. Even though it generates a different set of parameters, the general features like the opening of band gap when introducing electron correlation and the localization of the vacancy and impurity state, which will be discussed later, are consistent with the current set of parameters. Therefore, we are confident in the use of this parameter set for our future calculations.

C. Gutzwiller method for the many-body Hamiltonian

Following Rice and Ueda [31], we shall use the Gutzwiller method to study the many-body Hamiltonian (17). The method is a variational approach. The constraint condition of Eq. (19), to exclude state at any H site, is replaced by a set of renormalization factors.

We consider a variational ground state wavefunction $|\Psi\rangle$ which is of the form

$$|\Psi\rangle = P|\Psi_o\rangle, \tag{23}$$

where $|\Psi_o\rangle$ is a state of the tight binding Hamiltonian with no constraint, and P is the projection operator to project all empty electron states on each H site,

$$P = \prod_i n^h_{i,\uparrow} n^h_{i,\downarrow}, \tag{24}$$

where i runs over all H sites and $n^h_{i,s} = h^\dagger_{i,s} h_{i,s}$.

The ground state energy is given by

$$E_g = \langle H \rangle = \frac{\langle \Psi | H | \Psi \rangle}{\langle \Psi | \Psi \rangle}. \tag{25}$$

To calculate $\langle H \rangle$, we use the Gutzwiller method to compute the average values of each term in H in the state $|\Psi\rangle$. The Gutzwiller method is a static approximation, and the average of a local operator Q in the state $|\Psi\rangle$ is related to its corresponding average in the $|\Psi_o\rangle$ by a renormalized numerical factor g_Q, namely,

$$\langle Q \rangle = g_Q \langle Q \rangle_o, \tag{26}$$

where $\langle Q \rangle$ and $\langle Q \rangle_o$ are the average in the states $|\Psi\rangle$ and $|\Psi_o\rangle$ respectively.

In the present case, we have

$$\begin{aligned} \langle h^\dagger_{i,s} h_{j,s} \rangle &= \sqrt{g_i g_j} \langle h^\dagger_{i,s} h_{j,s} \rangle_o, \\ \langle d^\dagger_{i,\alpha,s} h_{j,s} \rangle &= \sqrt{g_j} \langle d^\dagger_{i,\alpha,s} h_{j,s} \rangle_o. \end{aligned} \tag{27}$$

The Gutzwiller factor g is calculated by counting the number of possible configuration in $|\Psi\rangle$ and in $|\Psi_o\rangle$, respectively. The value of g_i is

$$g_i = \frac{1 - n_i^{hole}}{1 - n_i^{hole}/2}, \tag{28}$$

where n_i^{hole} is the occupation number of holes at the H site i. Here we define a hole as an electron vacancy in a H^- ion and therefore

$$n_i^{hole} = 2 - \sum_{i,s} h^\dagger_{i,s} h_{i,s}.$$

The constraint Eq. (19) now disallows doubly occupied hole configurations on H sites. This leads to an effective Hamiltonian for the lanthanum hydrides,

$$H_{eff} = H'_h + H_{La} + H'_{mix} - \mu \sum_{i,s} h^\dagger_{i,s} h_{i,s}. \tag{29}$$

In the above equation, H_{La} is given by Eq.(20), and H'_h and H'_{mix} have the same form of H_h and H_{mix} in Eq.(18) and (21). The constraint condition is released, and the hopping integrals are renormalized to values

$$\begin{aligned} t^h_{i,j} &\to \sqrt{g_i g_j} t^h_{i,j}, \\ V_{i,\alpha,j} &\to \sqrt{g_j} V_{i,\alpha,j}. \end{aligned} \tag{30}$$

H hopping integrals $t^h_{i,j}$ are the values obtained from our local model including the crystal field effect. Furthermore, the atomic energies ϵ^h_i are shifted to $\epsilon^h_i - \epsilon_b$, where ϵ_b is the binding energy of the outer electron in a H^- ion. We use the free space value $\epsilon_b = 0.7$eV. Note that the outer electron in LDA is unbound [27]. μ Eq. (29) is an effective "chemical potential" [31]. The value of μ is determined by minimizing the total energy of the system

$$E_g = \langle H_{eff} + \mu \sum_{i,s} h^\dagger_{i,s} h_{i,s} \rangle_o. \tag{31}$$

In the lanthanum hydrides, the total energy is found to be insensitive to values of $\mu \simeq 0$, so we set $\mu = 0$. This is primarily due to the fact that ϵ^h is lower than ϵ^α.

To compare with heavy fermion systems, we may perform an electron-hole mapping for the lanthanum hydride model Hamiltonian, $\epsilon^h \to -\epsilon^h$, $\epsilon^\alpha \to -\epsilon^\alpha$, and the constraint is to project out doubly occupied hole states on H sites. In the hole notation, the "f" level in lanthanum hydrides is above the conduction bands. Therefore the hydrides are in the mixed valence, instead of the Kondo limit of the Anderson lattice model.

H_{eff} is a single particle Hamiltonian, and can be readily solved by analytic or numerical means. The Gutzwiller factor g_i, given by Eq.(28), satisfies a self-consistent equation for the electron occupation at H site i,

$$n^h_i = \langle n^h_i \rangle = \langle n^h_i \rangle_o. \tag{32}$$

Since $0 \le g \le 1$, the hopping integrals are then renormalized to smaller values. Hence the hydrogen band width is expected to be further reduced as a consequence of the correlation.In general g is position dependent. In the periodic cases such as in LaH_2 and LaH_3, g depends only on whether it is on the tetrahedral or octahedral site. For the inhomogeneous impurity states, g are strongly site dependent.

Note that this occupation related correlation is different from the intrasite electron-electron correlation we discussed in section II B. There the interaction between electrons on the same H^- ion was considered, and the result is the correlated wavefunction of two electrons on the same site. Here in this section we consider the correlation effect on the intersite hopping, which is a constraint on the every H-site.

IV. ELECTRONIC STRUCTURE OF LAH_2 AND LAH_3

We are now in position to calculate the electron spectrum of lanthanum hydrides. In this section, we consider LaH_2 and LaH_3.

In the case of LaH_2, all tetrahedral hydrogen sites are occupied, and all octahedral H sites are unoccupied. Because of the equivalence between the two tetrahedral H atoms in the unit cell, we need to introduce only one Gutzwiller factor, g_t. The energy spectrum, or the band structure, obtained from the H_{eff}, is plotted in Fig. 9. The two lower bands are primarily H^- bands, and are

fully filled, leaving one electron per unit cell in the bands of primarily La-5d characters. The Fermi energy is within the La-5d conduction bands, so that LaH_2 is a metal as expected. The correlations in LaH_2 do not change this qualitative property.

In LaH_3, all octahedral H sites are also occupied. We use two independent Gutzwiller factors g_t and g_o corresponding to the tetrahedral and octahedral sites respectively. The Gutzwiller factors are found to be $g_t = 0.78$, $g_o = 0.70$, which indicates the reduction of the hopping parameters between two H sites and between H and La sites. The electronic structure for LaH_3 is plotted in Fig. 10.

We find that LaH_3 is an insulator. The optical gap is found to be 1.5 eV or 2.1 eV depending on whether the crystal field is included in the estimate of the H-H hopping integrals as discussed in section II. The opening of the energy gap at the chemical potential is primarily due to the strong electron correlations in the H^- ions, which reduces the H^- band width. The large electron-electron Coulomb repulsion on the H^- ion also restricts the electronic state to exclude the empty electron state at any H-site, which further reduces the H^- band width. The energy of the conduction band at X-point seems too low, and is presumably due to the inaccuracy in the tight-binding fit, see Fig. 7(a) and 8(a).

The present method is an improvement of our previous work [16]. In that paper, we focused on the H bands and neglected the La bands. That is to assume that all the three lower bands, which is of primarily H-1s character and mixed with the La-5d orbitals, are purely H bands. Mathematically, the previous model is equivalent to the effective Hamiltonian Eq. (29) but without the renormalization factors (i.e. $g_i = 1$). The more sophisticated method presented here predicts a larger gap, closer to the observed value.

It would be interesting to study the band gap in LaH_3 as a function of the lattice constant a_o. As the lattice constant decreases, the electron hopping matrix elements between H-ions increase, and thus the H^- band width increases, possibly leading to the reduction of the gap and eventually to the closing of the gap. Therefore we expect a transition from insulator to a metal in LaH_3 under pressure. With the knowledge of the distance dependence of the hydrogen couplings t_1 and t_2, crystal field effect ($\propto 1/a_0$) and the orbital coupling parameters ($V_{dd\pi}$ and $V_{dd\sigma} \propto 1/a_0^5$, $V_{sd\sigma} \propto 1/a_0^{7/2}$) [40], we can calculate the evolution of the band gap as a function of a_0. We find that the band gap closes and LaH_3 becomes metallic when a_0 decreases by 11% to $0.89a_o$. (Fig. 11).

V. IMPURITY AND VACANCY STATES

In the previous two sections, we argued that electron correlation is the missing element from the LDA calculations, which failed to predict the insulating properties of the trihydrides. By introducing an electron correlation on H_2^- ions, we have found that LaH_3 is an insulator, consistent with experiment. However, more interesting physics lies in the mechanism of the metal-insulator transition in LaH_x. We can understand the transition by approaching it from either metallic ($x = 2$) and insulating ($x = 3$) end points. We investigate the former first.

A. An extra H atom in LaH_2

The introduction of a neutral H atom into a H_{oct} site in LaH_2 creates a s=1/2 magnetic impurity, which couples to the conduction electron spins. Let us study this impurity problem more carefully. First we consider the atomic limit and neglect the hybridization between the H-1s and La-5d orbitals. Then a conduction electron (La-5d) moves to the neutral H atom at H_{oct} site to form a H^- ion. Including the hybridization between H and La orbitals, the outer electron in the H^- ion will fluctuate between the H_{oct} site and the surrounding La sites. Since H^- ion is a spin singlet of two electrons, the coupling between H_{oct} and La orbital is antiferromagnetic. The effective Hamiltonian for the extra H atoms at H_{oct} is an antiferromagnetic Kondo model,

$$\mathcal{H}_{\rm imp} = \sum_{\mathbf{k},\alpha,s} \varepsilon_\alpha(\mathbf{k}) d^\dagger_{\mathbf{k},\alpha,s} d_{\mathbf{k},\alpha,s} + J \sum_i \mathbf{S}_i \cdot \mathbf{s}_i, \quad (33)$$

where i runs over all the occupied H_{oct}, $\mathbf{S}$ and $\mathbf{s}$ are the electron spins of the neutral H atom and of the conduction electron (annihilation operator $d_{\mathbf{k},\alpha,s}$ with energy $\varepsilon_\alpha(\mathbf{k})$) states. Because of the symmetry, only the two e_g La-5d orbitals are coupled to the 1s-H_{oct} electron directly. The exchange coupling will be large, $J \sim 0.7$ eV is in free space [32]. To estimate J in the hydrides, we use a local model including six neighboring La atoms around the H_{oct} site (Fig. 12). The dynamics is given by a 2×2 matrix Hamiltonian

$$\begin{pmatrix} \epsilon_{oct} & \sqrt{6}V \\ \sqrt{6}V & \bar{\epsilon}_d \end{pmatrix}, \quad (34)$$

where ϵ_{oct} is the atomic energy of the 1-s H_{oct} and $V = V_{sd\sigma}^{La-o}$ is the hybridization between the H_{oct} and each La. $\bar{\epsilon}_d$ is the energy of the combination of the six 5d-La-e_g orbitals around the H_{oct}, denoted by

$$|imp\rangle = \frac{1}{\sqrt{6}} \sum_i |e_g^i\rangle, \quad (35)$$

where $|e_g^i\rangle$ is the e_g orbitals as shown in Fig. 12 at the La site i. Using the Hamiltonian H_{La} in Eq. (20), we find the energy of $|imp\rangle$ is to be given by

$$\begin{aligned} \bar{\epsilon_d} &= \langle imp\,|H_{La}|\,imp\rangle, \quad (36) \\ &= \epsilon'_d + \epsilon_{Kin}. \end{aligned}$$

ϵ_{Kin} is the kinetic energy of the electron in the $|imp\rangle$,

$$\epsilon_{Kin} = 4t^{e_g-e_g} = \frac{V_{dd\sigma}}{4} - 3V_{dd\pi}, \quad (37)$$

where $t^{e_g-e_g}$ is the hopping integral between two La-e_g states whose orbitals point to the central H_{oct}. From Eq. (34), we find the spin-singlet state energy to be

$$\epsilon_{s=0} = \frac{1}{2}\left[(\epsilon_{oct}+\bar{\epsilon}_d) - \sqrt{(\epsilon_{oct}-\bar{\epsilon}_d)^2 + 24V^2}\right]. \quad (38)$$

Using the parameters fitted to the LDA, $\epsilon_{oct} = -3.3$ eV, $\bar{\epsilon_d} = -0.7$ eV, $V = -1.2$ eV, we have $\epsilon_{s=0} = -5.21$ eV. This energy should be compared with the chemical potential ($\mu = -0.62$ eV, see Fig. 9) for a spin triplet state, in which an electron with the same spin is placed at the Fermi level conduction band. Therefore, we arrive at a value

$$J = \mu - \epsilon_{s=0} = 4.59 \text{ eV}. \quad (39)$$

In this Kondo description conduction electrons are captured by the neutral H atoms at H_{oct} sites to form tightly bound singlets. In this description the material with all octahedral sites occupied, LaH_3, is viewed as a Kondo insulator with a large band gap. Our conclusion here is consistent with Eder *et al.* [17]. The actual gap in the insulator is expected to be reduced from the value in Eq. (39) obtained within an impurity calculation.

B. Localized vacancy state in LaH_3

Next we examine the transition starting from insulating LaH_3. The removal of neutral H atoms introduces vacancies at octahedral sites H^V_{oct} which donate an electron to the conduction band. In a conventional semiconductor such as in the phosphorus-doped silicon (Si:P), the impurity state is described by an effective mass theory, and the result is a hydrogen-like bound state with a large effective Bohr radius a^*_B of order ~ 100 Å due to the light effective electron mass and the large dielectric constant. The critical impurity concentration δ_c at which the system becomes metallic is given by Mott criterion $\delta_c \sim (l/a^*_B)^3$, where l is the inter-atomic distance. Because of $a^*_B \gg l$, δ_c is very small (10^{-3} for Si:P). The vacancy state in $LaH_{3-\delta}$ is very different, however. Experimentally, it is found that the semiconducting states extend to $\delta_c = 0.25$ for $LaH_{3-\delta}$, and to even larger value for yttrium hydrides [1,11]. This suggests a very localized impurity state. In our previous short paper we proposed the vacancy state in $LaH_{3-\delta}$ to be a very localized La-5d-e_g orbitals centered at the vacancy with s-wave symmetry, and we used perturbation theory to estimate its energy in support of our proposal. Here we calculate the lowest vacancy state and further support our previous vacancy model.

Let us begin with a qualitative argument and a simple estimate. The La-5d-e_g and H_{oct} electrons hybridize strongly to form bonding (mainly H) and antibonding (mainly e_g) states. The underlying physics may be simply described by the local model of a single H_{oct} atom surrounded by six La atoms (see last section). The bonding state energy is given by Eq. (38), and the anti-bonding state energy is

$$\epsilon_{ab} = \frac{1}{2}\left[(\epsilon_{oct}+\bar{\epsilon}_d) + \sqrt{(\epsilon_{oct}-\bar{\epsilon}_d)^2 + 24V^2}\right]. \quad (40)$$

A vacancy of H_{oct} breaks the bonds locally and the e_g electron becomes locally non-bonding, which has much lower energy than the antibonding e_g states away from the vacancy. Therefore, in addition to serving as a positive charge center as in conventional n-type semiconductors, H^V_{oct} creates a potential well for the e_g state electron. The latter is non-perturbative, and is responsible for the unusual concentration dependence of the semiconductor.

Consider a s-symmetric octahedral e_g state (S-state hereafter) around a H^V_{oct} as shown in Fig. 13. The H^V_{oct} vacancy breaks the bonds on the octahedron and reduces the antibonding energy of the S-state. This S-state is very localized because the neighboring octahedral s-state is antibonding and has a much higher energy. We can estimate the depth of the potential well, V_0. The vacancy state (the non-bonding state) energy is

$$E_{vac} = E_{nb} = \bar{\epsilon}_d. \quad (41)$$

Therefore $V_o = E_{ab} - E_{nb}$ is given by

$$V_o = \frac{1}{2}\left[\epsilon_{oct} - \bar{\epsilon}_d + \sqrt{(\epsilon_{oct}-\bar{\epsilon}_d)^2 + 24V^2}\right]. \quad (42)$$

The numerical value of the potential well is $V_o = 1.9$ eV.

From Eq. (41), we estimate $E_{nb} = -0.7$ eV, below the lowest La-5d-t_{2g} band which has energy zero as we can see from Fig. 10(a).

In the above estimate for the energy of the localized vacancy state, we have not included a Coulomb attraction between the H_{oct} vacancy and the extra electron. This attraction will further lower the vacancy state energy. We conclude that the H_{oct}-vacancy electron state is highly localized and it is well within the band gap. The localized vacancy state here is similar to the carbon vacancy state in TiC, where the C-vacancy leads to a well localized impurity states [33]. We emphasize that the potential well generated by the H_{oct} vacancy is primarily short-ranged, different from the ideal long-range Coulomb force. The effective radius of the impurity state is only half of the lattice constant.

The existence of localized vacancy state can be verified by a finite size calculation for a single H_{oct} vacancy in LaH_3, an improvement of the local model discussed above. The system is described by Hamiltonian (17)-(28) with all but one H_{oct} occupied. We use the Gutzwiller method given in section III C to study the vacancy state. The vacancy breaks the translational invariance; the Gutzwiller factor g_i now depends on the site,

and has only crystal group symmetries with respect to the vacancy state. Because of its localized nature, we can study the vacancy state in a finite-size system. The problem then can be solved explicitly using the Gutzwiller approximation. We consider a small cubic of $3 \times 3 \times 3a_o^3$ lattice in the calculations. We choose the vacancy site to be at the center of the lattice. An S-state around the vacancy site is found, as we expected. All the surrounding La atoms have their $5d$ e_g orbitals pointing towards the vacancy and have the same weighting factor. The t_{2g} orbitals, however, have no contribution in the S state. It is found that the S state has an energy $E_{vac} = -0.38$ eV below the $5d$ La conduction band at Γ point which is a t_{2g} state and is decoupled from the vacancy state. Therefore, electrons will occupy the less energetic vacancy state instead of the conduction band, implying an insulating ground state for $x \leq 3$. When more vacancies are added, more localized states are formed within the band gap and the material will become metallic when localized states start to substantially overlap with each other.

In Table V we list the probability of the vacancy state at different atomic sites in the lattice. As we can see, the state is largely distributed in the six neighboring La sites with the probability of 58%. This clearly shows its localized nature.

The localized nature of the vacancy state in LaH_x is consistent with the temperature dependence of the d.c. resistivity data at room temperatures, which has a temperature depedence consistent with variable range hopping [11]. Localized states are a prerequisite for variable range hopping. In the next section we will discuss the electronic band width of the vacancy states.

C. Effective electron hopping integrals between two vacancies

In LaH_3, octahedral hydrogens are not fixed in position but able to move around by diffusion. Electrons in the vacancy state, of course, are strongly bound by the Kondo like effect as discussed before. Therefore, a calculation of the vacancy-vacancy interaction and the effective electron hoppings between the two H_{oct}^{V} is necessary to the electronic band of the vacancy states. We estimate here the effective hopping integrals between two H_{oct}^{V} sites.

The effective hopping integral t_{v-v} between the two H_{oct} vacancy sites is given by

$$t_{v-v} = \langle \Psi_1 | H' | \Psi_2 \rangle,$$

where H' is the inter-atomic Hamiltonian given by H in Eq. (17). $|\Psi_1\rangle$ and $|\Psi_2\rangle$ are the electron state of the two vacancy sites.

Note that the vacancy states $|\Psi_\alpha\rangle$ are basically linear combinations of the nearest 6 La-$5d$-e_g orbitals (Fig. 14). For simplicity, we model the vacancy state by the local description as shown in Fig. 13, and only the n.n. coupling between La-sites in H', and hence $V_{dd\sigma}$ and $V_{dd\pi}$, will be considered while contributions from further distant orbitals is negligible. We apply the fitted values of $V_{dd\sigma}$ and $V_{dd\pi}$ from section III. Table VI lists the values of hopping integral of vacancy states separated by different distances.

It is interesting to notice that the value of the hopping integral oscillates when the distance increases. A more careful investigation tells us that the hopping of the vacancy state within the same cubic sublattice is larger in value and negative in sign. In La hydrides H_{oct} sites forms a face-center cubic lattice, which can also be divided into 4 interlocking simple cubic sublattices. Our finding shows the hopping within the same sublattice is more probable than between different sublattices.

The precise nature of the transition in optical properties is not yet well understood. Since the vacancy states are highly localized, the vacancy concentration at the metal insulator transition of a random vacancy distribution is quite high. Hence the mobile carrier density is high. This explains why the metallic phase is a good metal with high reflectivity.

One aspect of the hydride system is unique, namely the existence of an order-disorder transition among the vacancies which enables one to separate the effects of disorder and Coulomb interaction in the electronic band of vacancy states. Usually donors and acceptors are fixed in doped semiconductors so that this is impossible. The disordered vacancy phase is insulating with variable range hopping among the localized vacancy states. Interestingly Shinar *et al.* [11] reported a transition to an ordered vacancy phase at temperatures around 250°K for concentrations $x \sim 2.8 - 2.9$ and metallic d.c. conductivity in the ordered phase. This shows that Anderson localization is responsible for the insulating character of the disordered phase. However in the ordered phase there must be a Mott transition to an insulator as the vacancy density is lowered. It would be very interesting to examine this region and look for the Mott transition in an ordered vacancy sublattice.

VI. PHYSICAL PROPERTIES OF INSULATING $LAH_{3-\delta}$

In order to study the electronic structure of metal hydrides, various measurements, such as photoelectron and optical spectroscopy, have been performed for metal hydrides with different hydrogen concentration. From these experiments [36] interband excitations can be measured and compared to theoretical band structure. Their data can be used to verify the accuracy of theoretical prediction for the electronic structure. Most theoretical investigations have been done on the dihydrides and trihydrides, while hydrides with intermediate hydrogen concentration are difficult to study. In this section we will discuss some

physical properties predicted from our theory in connection with the existing or further experiments.

A. Magnetic properties of $LaH_{3-\delta}$

The vacancy state is a localized object of spin-1/2 as discussed in section V B. Near the trihydride phase, $LaH_{3-\delta}$ is an insulator for small δ. The vacancies have a tendency to be singly occupied because two electrons on the same vacancy site repel each other. The magnetic susceptibility is expected to follow a Curie law with a linear inverse temperature dependence.

B. Density of states

Peterman *et al.* [36] studied the composition-dependent electronic structure of LaH_x, $1.9 \leq x \leq 2.9$, using photoelectron spectroscopy with synchrotron radiation (10 eV $\leq h\nu \leq$ 50 eV). Fujimori *et al.* [37] on the other hand studied the electronic structure of yttrium hydride by x-ray photoemission spectroscopy. Here we compare our calculated densities of states with the experiment on lathanum hydrides, as shown in Fig. 15.

We performed a finite size calculation with lattice size of $15 \times 15 \times 15 a_0^3$ based on the model Hamiltonian (17). Numbers of states in the band structure of LaH_3 and LaH_2 are counted as a function of energy. The discrete densities of states were smoothed out by replacing delta peaks with Lorentzian distribution curve of width $\Gamma = 0.3$ eV. Our results for LaH_2 and LaH_3 are similar to the previous theoretical calculations by Gupta and Burger [36,38]. In Fig. 15, the pronounced two-peak structure is associated with the flat region of hydrogen bands near symmetry points X, L, K (refer to the band structure Fig. 9 and 10) while the small bump at the zero energy in LaH_2 is associated with the La band near symmetry points W and K. Experiments showed that the small bump shrinks as hydrogen concentration increases and eventually disappears when the sample approaches the trihydride. However Gupta and Burger expected a metallic state for LaH_3 from their LDA calculation which ignored electron correlation. In our calculations, the density of states goes to zero at -2.2 eV, indicating an insulating behavior for LaH_3. However, the calculated widths for LaH_2 and LaH_3 are considerably smaller than the experiment results, a discrepancy similar to that in the LDA . The experimental data also shows a shift of the lowest energy peak when the concentration increases. The positions of calculated peaks do not significantly depend on the concentration and does not agree to the experiment. The origin of these discrepancies is not clear. Since our theory uses some parameters extracted from LDA, similar features except for the band gap may be expected from both theories.

C. Optical Conductivity

The optical absorptivity spectra for samples of LaH_x and NdH_x were also measured by Peterman *et al.* [36] at 4.2K at near-normal incidence. From the absorption data, they deduced the real and imaginary part of the dielectric constant, and hence the optical conductivity by using Kramers-Kronig analysis. They found a relatively broad feature for $LaH_{2.87}$. However, their samples were polycrystals and the use of Kramers-Kronig analysis might enlarge the data uncertainties. On the other hand, a more recent and accurate measurement reported by Griessen *et al.* [39] sheds new light on the optical conductivity curve. The optical transmission spectra of the insulating phase $YH_{3-\delta}$ were measured as functions of the photon frequency $\hbar\omega$ and of hydrogen vacancy concentration δ. The effect of the vacancy appears to reduce the overall transmission spectra quite evenly between $\hbar\omega = 0.5$ eV and 2 eV. In our theory, the δ-dependent conductivity $\sigma(\omega)$ at $\hbar\omega < 2.8$ eV mainly determined by the optical transition from the vacancy state to the conduction bounds. The transition energy from the valence bands to the vacancy state is larger because of the larger energy difference between the two states and because of the Coulomb repulsion of the doubly occupied electron states on the same vacancy site. Since the vacancy state is highly localized, the transition matrix largely depends on the density of states of the conduction bands, which is expected to lack pronounced feature.

Within the dipole approximation, the real part of conductivity contributed from the vacancies is given by

$$\sigma(\omega) = const \times \omega \sum_n |\langle n|x|vac\rangle|^2 \, \delta(E_n - E_{vac} - \hbar\omega) \tag{43}$$

where $|vac\rangle$ is the vacancy state. The sum is over all conduction states $|n\rangle$. We shall use a local model to describe $|vac\rangle$, as shown in Fig. 13,

$$|vac\rangle = \sum_{\mathbf{R}_{La},\alpha} a_\alpha(\mathbf{R}_{La}) |\mathbf{R}_{La}, d_\alpha\rangle, \tag{44}$$

where $\mathbf{R}_{La}$ denotes the position of the 6 La atoms and d_α the $5d$-e_g orbitals, and $a_\alpha(\mathbf{R}_{La})$ are the wavefunction amplitudes. The conduction bands are mainly $5d$-La character mixed with $1s$-H orbitals. The La intraband transition is a difficult case to calculate with the unknown transition matrices involved. For simplicity and for the purpose of illustration, here we consider the part of the optical transition to the conduction bands with the H_{tet} character, and assume the transition matrix is non-zero only between the La-$5d$ and to its neighboring H_{tet} orbitals.

$$|n\rangle = \sum_{\mathbf{R}_t} b_n(\mathbf{R}_t) |\mathbf{R}_t, s\rangle, \tag{45}$$

Let $|\mathbf{R}_t, s\rangle$ be the $H_{\rm tet}$ $1s$ state at site $\mathbf{R}_t$, and $b_n(\mathbf{R}_t) = \langle \mathbf{R}_t, s|n\rangle$ the amplitude of the state $|\mathbf{R}_t, s\rangle$ in $|n\rangle$, we then have

$$\langle vac\,|x|\,n\rangle = \sum_{\mathbf{R}_{La},\mathbf{R}_t,\alpha} a^*_\alpha(\mathbf{R}_{La}) b_n(\mathbf{R}_t) \langle \mathbf{R}_{La}, d_\alpha\,|x|\,\mathbf{R}_t, s\rangle, \tag{46}$$

where the sum over $\mathbf{R}_t$ runs all the neighboring $H_{\rm tet}$ of the six La sites. We calculate The $a^*_\alpha(\mathbf{R}_{La})$ and $b_n(\mathbf{R}_t)$ by numerically solving a finite size cell $(15 \times 15 \times 15 a_0^3)$ of LaH_3 with a single $H_{\rm oct}$ vacancy. The orbital overlap $\langle d_\alpha|x|s\rangle \propto \langle d_\alpha|p_x\rangle$ is a linear combination of the coupling parameters $V_{pd\sigma}$ and $V_{pd\pi}$ and can be found in Harrison's book [40]. It is estimated the ratio $V_{pd\sigma}/V_{pd\pi} \simeq -2.17$. The optical conductivity $\sigma(\omega)$ can thus be calculated up to an overall constant. In the calculations, we use a rigid band approximation, where the conduction band spectra is unaffected by the vacancy. This approximation is justified by comparing the result to the actual conduction band in the presence of the vacancy from the finite size calculation. Only minute deviation is observed in small size calculation.

The calculated result (Lorentzian width 0.5 eV) is showed in the Fig. 16 which gives a fairly featureless curve. Except the small peak around 4 eV, the curve does not show any pronounced features. This is qualitatively consistent with the experiments [36,6].

There is a threshold $\sim E_c$ in $\sigma(\omega)$, which is the energy cost for the vacancy state to transfer to the conduction band. In our calculation, $E_c \simeq 0.1$ eV. This small value is due to the inaccurate tight-binding fitting to the LDA, resulting in lower energy at X-point in LaH_3. If we subtract this, $E_c \simeq 0.38$ eV. In our estimate, a charged Coulomb attraction has not been added, so that the actual threshold is larger.

It is interesting to compare the optical properties of the hydrides vacancy state with those of the usual doped semiconductors studied by Thomas *et al* [41]. First we note an important difference between the two systems. In a conventional semiconductor, the hydrogen-like $1s$ groundstate has an electronic dipole active transition to the bound $2p$ state, leading to optical absorption peaks at about 30 meV in Si. In the metal hydrides, the ground state of a vacancy is a highly localized s-wave-like state (see Fig. 13).

However, the p-wave-like state is expected to be only weakly bound with much larger spatial distribution. This is because of the absence of short-range attraction as in the s-wave state. The long range Coulomb attraction between the electron and the vacancy induces a bound p-wave state with a larger radius similar to the hydrogen-like ones. Therefore we expect only a weak dipole transition intensity from the very localized s-wave state (mainly induced by the short range bonding force) to the p-wave state. The absence of the short-range force in the p-wave vacancy state can be explained as follows. Consider a local p-wave-like state of La-$5d$ orbits, similar to that in Fig. 13 except for the symmetry that is changed from s- to p-wave-like. By symmetry, the p-wave-like state is decoupled to the $1s$ electron state of the center hydrogen atom. Note that this property of the vacancy state is markedly different from that of the negative ion vacancy in an alkali halide crystal. The latter is called a color center that has one excess electron bound at the vacancy [42]. The potential created by the vacancy in alkali halides is a long-range Coulomb force, and the color center absorbs visible light in a dipole transition to a bound excited state of the center. Our theory for the vacancies in hydrides predicts much weakness of such transitions.

VII. CONCLUSION

In this paper, we have examined the importance of the electron correlation in negatively charged ions (H^- ions), and identify the metal hydrides to be a strongly correlated system. We develop a many-body theory to describe the H^- ion lattice in hydrides. We use lanthanum hydrides as a prototype for these compounds and show that LaH_2 is a metal, and LaH_3 is a band insulator where the electron correlation plays a crucial role.

The electronic structure for metal hydrides is described by the large U-limit Anderson lattice model. The parameters for the hydrides are determined by a combination of method including the microscopic calculations for the electron hopping integrals between hydrogen sites and parameter value obtained from LDA methods for La/H hybridization. The Anderson lattice model is then solved using a many-body technique − Gutzwiller method. The elementary entity when a H atom is removed from the insulating LaH_3 is the octahedral hydrogen vacancy, which is highly localized electronically, due to the strong hybridization between the H-$1s$ and its neighboring La-$5d$-e_g orbitals. This explains why the metal-insulator transition can occur at a large vacancy concentration $\sim 25\%$.

Our theory for the localized vacancies in hydrides predicts a much weak optical transition to the hydrogen-like-$2p$ state in comparison with observed transitions in conventional semiconductors.

VIII. ACKNOWLEDGMENT

We thank Prof. R. Griessen, O. Gunnarsson for many useful discussions. This work was in part supported by DOE grant DE/FG03-98ER45687, and by Russian Foundation for Basic Research grant RFFI-98-02-17275. KKN, FCZ and VIA would like to thank the Zentra for the Studies of ETH for support during their visit to ETH where this project was started. FCZ and KKN wish to acknowledge the URC support from University of Cincinnati.

[1] J.N. Huiberts, R. Griessen, J.H. Rector, R.J. Wijngaarden, J.P. Dekker, D.G. de Groot, and N.J. Koeman, Nature **380**, 231 (1996).

[2] For a review on hydrides, see P. Vajda, Hydrogen in Rare-Earth Metals including RH_{2+x} Phases, in "Handbook on the Physics and Chemistry of Rare Earths", Vol. 20 (Elsevier Science 1995), 207, and references therein.

[3] P. van der Sluis, M. Ouwerkerk, and P.A. Duine, Appl. Phys. Lett. **70**, 3356 (1997).

[4] L. Degiorgi *et al*. Phys. Rev. B44, 7808 (1991).

[5] J.N. Huiberts, R. Griessen, R.J. Wijingaarden, M. Kremers, and C. Van Haesendonck, Phys. Rev. Lett. **79**, 3724 (1997).

[6] R. Griessen, private communications (1997).

[7] E. Wigner and H.B. Huntington, J. Chem. Phys. **3** 764 (1953).

[8] G.E. Study and R.N.R. Mulford, J. Am. Chem. Soc. **78**, 1083 (1956).

[9] A. Pebler and W.E. Wallace, J. Phys. Chem. **66**, 148 (1962).

[10] D.K. Misemer and B.N. Harmon, Phys. Rev. **B26**, 5644 (1982).

[11] J. Shinar, B. Dehner, R.G. Barnes, and B.J. Beaudry, Phys. Rev. Lett. **64**, 563 (1990).

[12] A.C. Switendick, Solid State Commun. **8**, 1463 (1970).

[13] J.P. Dekker, J. van Ek, A. Lodder, and J.N. Huiberts, J. Phys. Cond. Mat. **5**, 4805 (1993).

[14] Y. Wang and M.Y. Chou, Phys. Rev. Lett. **71**, 1226 (1993).

[15] V.I. Anisimov, private communications.

[16] K.K. Ng, F.C. Zhang, V.I.Anisimov, T.M. Rice, Phys. Rev. Lett. **78**, 1311 (1997).

[17] R. Eder, H.F. Pen, and G.A. Sawatzky, preprint (1997).

[18] X W. Wang and C. Chen, Phys. Rev. B **56**, 7049 (1997).

[19] P.J. Kelly, J.P. Dekker, and R. Stumpf, Phys. Rev. Lett. **78**, 1315 (1997).

[20] E. Chang and S. Louie, bulletin of APS, **43**, 170 (1998).

[21] H.A. Bethe and E.E. Salpeter, in "Handbuch der Physik Bd. 35", Edited by S. Flugge, Springer-Verlag, (1957).

[22] S. Chandrasekhar, Astrophys. J. **100**, 176 (1944).

[23] E.A. Hylleraas and J. Midtdal, Phys. Rev. **103**, 829 (1956).

[24] H.S. Taylor and F.E. Harris, J. Chem. Phys. **39**, 1012 (1963).

[25] I. Fischer-Hijalmars, Ark. Fys. **16**, 33 (1959). A similar method with a much less accurate wavefunction for H^- was used to study $E_\pm$.

[26] R.B. Laughlin, Phys. Rev. Lett. **50**, 1395 (1983).

[27] O. Gunnarsson, private communications.

[28] Gutzwiller M.C., Phys. Rev. Lett **10**, 159 (1963).

[29] Vollhardt D., Rev. Mod. Phys. **56**, 99 (1984).

[30] J.C. Slater and G.F. Koster, Phys. Rev. **94**, 1498 (1954).

[31] T.M. Rice and K. Ueda, Phys. Rev. Lett. **55**, 997 (1985).

[32] The bound H^--ion is a spin singlet electron state. We consider here the spin triplet electron state to be essentially non-bound.

[33] J. Redinger *et al*., J. Phys. Chem. Solids **46**, 383 (1985).

[34] C.G. Titcomb, A.K. Cheetham, and B.E.F. Fender, J. Phys. C **7**, 2409 (1974).

[35] V.K. Fedotov, V.G. Fedotov, M.E. Kost, and E.G. Ponyatovskii, Sov. Phys. Solid State **24**, 1252 (1982).

[36] D.J. Peterman, J.H. Weaver, D.T. Peterman, Phys. Rev. B **23**, 3903 (1981).

[37] A. Fujimori and L. Schlapbach, J. Phys. C, **17**, 341 (1984).

[38] M. Gupta and J.P. Burger, Phys. Rev. **B22**, 6074 (1980).

[39] R. Griessen, J.N. Huiberts, M. Kremers, A.T.M. van Gogh, N.J. Koeman, J.P. Dekker, P.H.L. Notten, J. Alloy Comp., **253**, 44 (1997).

[40] Walter A. Harrison (1980), "Electronic Structure and the Prosperites of Solids", W.H. Freeman and Company, Chapter 20.

[41] G.A. Thomas *et al*., Phys. Rev. B **23**, 5472 (1981).

[42] C. Kittel, "Introduction to Solid State Physics", John Wiley & Son, Inc. New York, 1986.

$d(a.u.)$	4	4.5	6
E_1(a.u.)	-0.25746	-0.22687	-0.16789
a_1	0.44324	0.39654	0.27863
a_2	0.08514	0.05775	0.01804
a_3	0.02785	0.01376	0.00146
b_1	-0.14039	-0.11154	-0.05866
b_2	-0.04145	-0.02566	-0.00748
b_3	-0.01609	-0.00731	-0.00123
t	-0.03611	-0.02857	-0.01346

TABLE I. Values of integrals in Eq. (10) and the hopping integrals $t(d)$ for different inter-proton distances d. All distances and energies are in atomic unit.

Cubic size (a_0)	Crystal field reduction (eV)
1	0.084674
2	0.145003
3	0.212051
4	0.223285
5	0.226712
6	0.230330

TABLE II. Change of t_1, the electron hopping integral between the n.n. tetrahedral H sites, due to crystal field effect of ions within a cube cell of various size. The change converges as the size of the cubic cell increases. a_o: lattice constant in LaH_3.

Parameters	fitting values
atomic energy of La $5d$ t_{2g}	$\epsilon_d = 1.6$
atomic energy of La $5d$ e_g	$\epsilon'_d = 1.4$
atomic energy of H_{tet}	$\epsilon_t = -3.2$
atomic energy of H_{oct}	$\epsilon_o = -2.6$
n.n. La-La π-bonding	$V_{dd\pi} = 0.6$
n.n. La-La σ-bonding	$V_{dd\sigma} = -1.2$
n.n.n. La-La π-bonding	$V'_{dd\pi} = -0.1$
n.n.n. La-La σ-bonding	$V'_{dd\sigma} = -0.2$
n.n. La-H_{oct} σ-bonding	$V_{sd\sigma}^{La-o} = -1.2$
nearest La-H_{tet} σ-bonding	$V_{sd\sigma}^{La-t} = -1.3$
nearest H_{tet}-H_{tet} σ-bonding	$t_{t-t} = -0.4$
nearest H_{oct}-H_{tet} σ-bonding	$t_{t-o} = -0.79$

TABLE III. Tight binding parameters extracted from the LDA results of Fig. 7 for LaH_3 and LaH_2. All the energies are in units of eV. The band structure of LaH_3 from the tight binding model of these parameters is plotted in Fig. 8.

Parameters	Renormalized values
nearest La-H_{oct} σ-bonding	$V_{sd\sigma}^{La-o} = -1.004$
nearest La-H_{tet} σ-bonding	$V_{sd\sigma}^{La-t} = -1.146$
nearest H_{tet}-H_{tet} σ-bonding	$V_{ss\sigma}^{t-t} = -0.228$
nearest H_{oct}-H_{tet} σ-bonding	$V_{ss\sigma}^{o-t} = -0.309$

TABLE IV. Renormalized parameters of Gutzwiller method for LaH_3.

type of atom	position (a_0)	distance (a_0)	weighting
H_{tet}	$(\frac{1}{4}, \frac{1}{4}, \frac{1}{4})$	0.4330	0.0012
H_{tet}	$(\frac{3}{4}, \frac{1}{4}, \frac{1}{4})$	0.8292	0.0365
H_{tet}	$(\frac{3}{4}, \frac{3}{4}, \frac{1}{4})$	1.0897	0.0002
H_{tet}	$(\frac{3}{4}, \frac{3}{4}, \frac{3}{4})$	1.2990	0.0134
H_{tet}	$(\frac{5}{4}, \frac{1}{4}, \frac{1}{4})$	1.2990	0.0087
H_{tet}	$(\frac{5}{4}, \frac{3}{4}, \frac{1}{4})$	1.4790	0.0012
H_{oct}	$(\frac{1}{2}, \frac{1}{2}, 0)$	0.7071	0.1426
H_{oct}	$(1, 0, 0)$	1.0000	0.0111
H_{oct}	$(1, \frac{1}{2}, \frac{1}{2})$	1.2247	0.0001
H_{oct}	$(1, 1, 0)$	1.4142	0.0004
La	$(\frac{1}{2}, 0, 0)$	0.5000	0.5790
La	$(\frac{1}{2}, \frac{1}{2}, \frac{1}{2})$	0.8660	0.0983
La	$(\frac{1}{2}, 1, 0)$	1.1180	0.0499
La	$(\frac{3}{2}, 0, 0)$	1.5000	0.0269

TABLE V. Weighting factors of the vacancy state at different atomic sites. The third column shows the total weighting of atomic sites which share the same distance from the vacancy site (origin). Only one position vector is shown in the second column for each distance while the others can be deduced from symmetry.

Vacancies separation (a_o)	Hopping integral (eV)
$\sqrt{2}/2$ (different s.l.)	0.475
1 (same s.l.)	-0.7
$\sqrt{3/2}$ (different s.l.)	0.125
$\sqrt{2}$ (same s.l.)	-0.175
$\sqrt{10}/2$ (different s.l.)	0.0625

TABLE VI. Calculated hopping integrals of vacancy state for various vacancies separation. Inside the parentheses are the indication of the two vacancies belonging to the different or the same sublattices (s.l.) of the fcc.

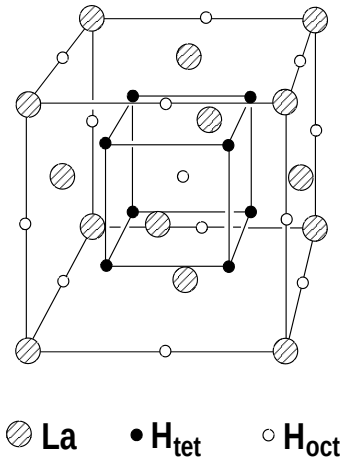

FIG. 1. Lattice structure (f.c.c) of LaH_x. As x increases from 2 to 3 the H-atom content at octahedral sites increases from empty to full, and a shiny metal evolves to an insulator.

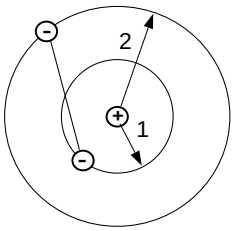

FIG. 2. Illustration of Chandrasakhar's wavefunction Eq. (1) for H^-, describing two electrons bound to a proton. The solid line between the two electrons represents the correlation term in Eq. (1).

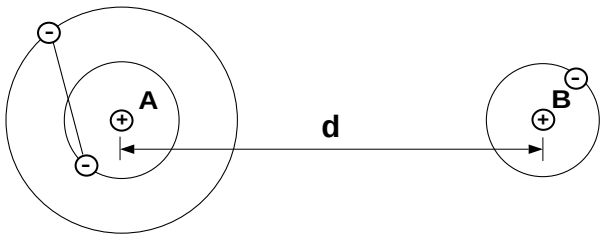

FIG. 3. Illustration of H_2^- ion, a system with two protons of distance d and three electrons. Shown at left is a H^- ion, described by the wavefunction of Eq. (1), and at right is a neutral H atom in the groundstate.

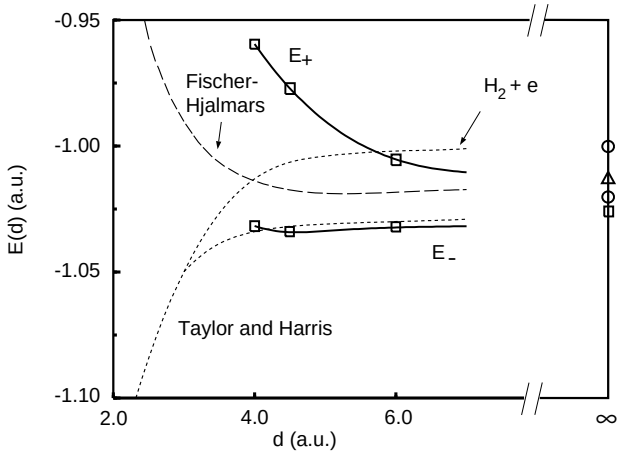

FIG. 4. Ground state energies (E_-, odd parity) and lowest energies of even parity state (E_+) in a H_2^- ion as a function of the two proton distance d. The lower (upper) solid line shows the present result for the bonding energy E_- (antibonding energy E_+) of the H_2^- ion. Dashed line is the E_- from Fischer-Hjalmars [25]. The lower dotted line is the E_- estimated by Taylor and Harris [24]. The upper dotted line shows the ground state energy of a H_2 molecule and a free electron for comparison. At $d \to \infty$, the energy is the sum of a H^- ion and a H atom, shown with a square from the present calculation, a triangle from Fisher-Hjalmars and the lower circle from Taylor and Harris. The upper circle is the energy of two independent H atoms and a free electron.

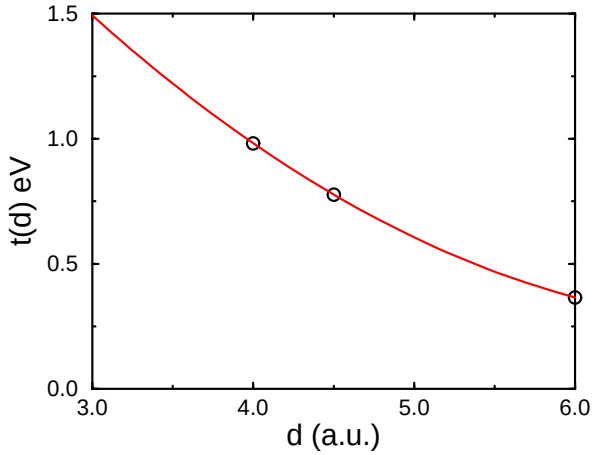

FIG. 5. Electron hopping integral $t(d)$ as a function of the distance d between two H ions. The hydrogen hopping integral decreases rapidly with increasing distance between the two H-ions. The equilibrium separation between the two nearest H_{tet}'s, and between neighboring H_{tet} and H_{oct} are 5.29 a.u. and 4.58 a.u., respectively. The solid line shown here is fitted to the three data points.

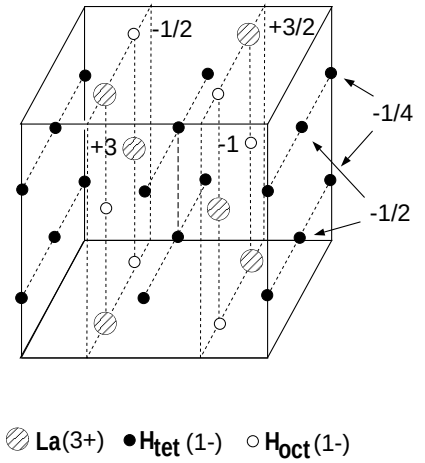

FIG. 6. A cubic cell with the center of H_2^- as the origin is shown. Total charges of ions enclosed in the cell are neutral. Charges in unit of e on an edge, surface and corner are counted as a quarter, half and eighth of the original charges respectively. Only a few examples are given in the figure. Dotted lines are guides to the eyes.

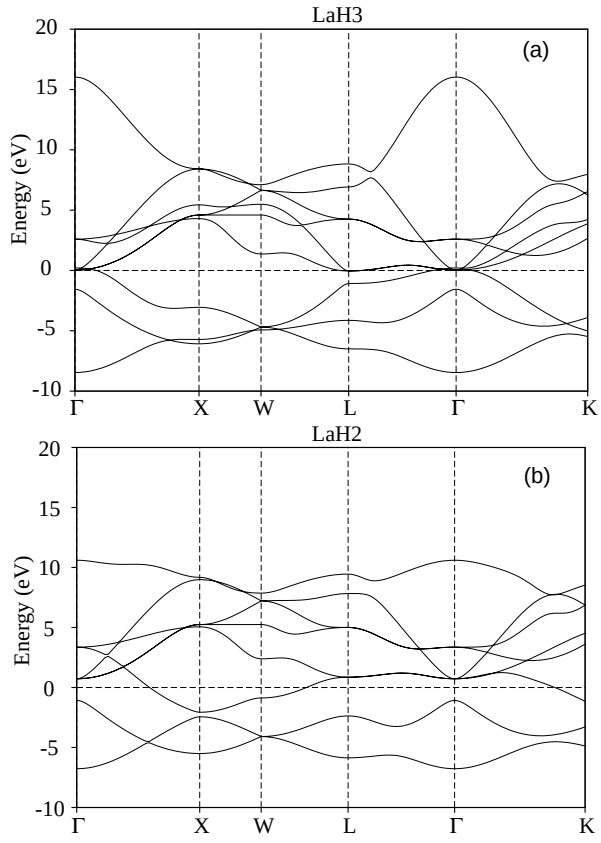

FIG. 7. Band structures of (a) LaH_2 and (b) LaH_3 from local density approximation calculation. The Fermi energy in LaH_3 is between the top of the H bands (the lower 3 bands) and the bottom of the La bands (upper 5 bands). $\Gamma = (0,0,0)$, X$= (2\pi,0,0)$, W$= (2\pi,\pi,0)$, L$= (\pi,\pi,\pi)$, K$= (3\pi/2,3\pi/2,0)$, in unit of $1/a_o$, are the high symmetry points in crystal momentum space.

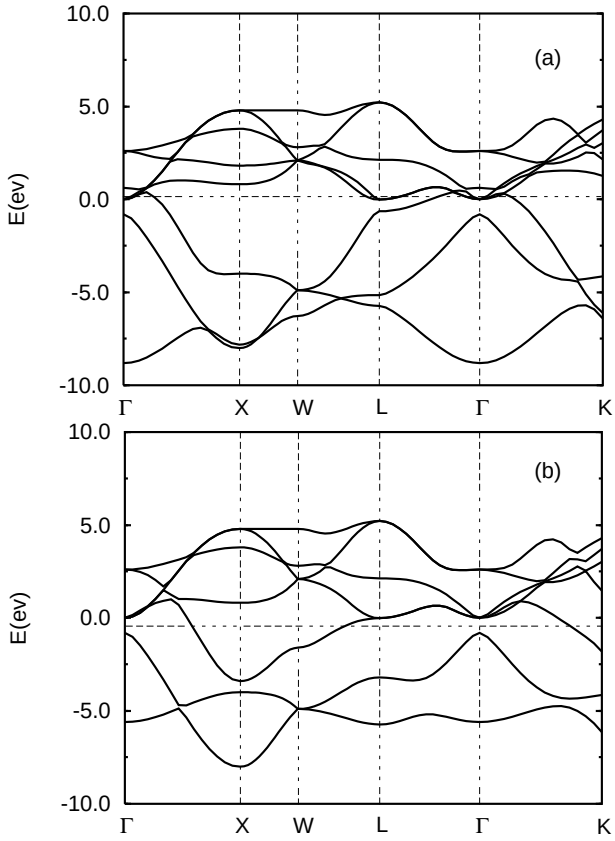

FIG. 8. The fitted band structures from the tight binding model with parameters listed in Table III for (a) LaH_3 and (b) LaH_2.

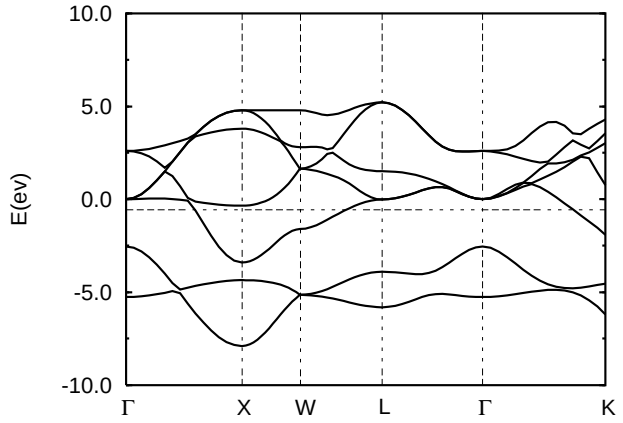

FIG. 9. The conduction and valence bands of LaH_2 calculated from model Hamiltonian (17) by using Gutzwiller method.

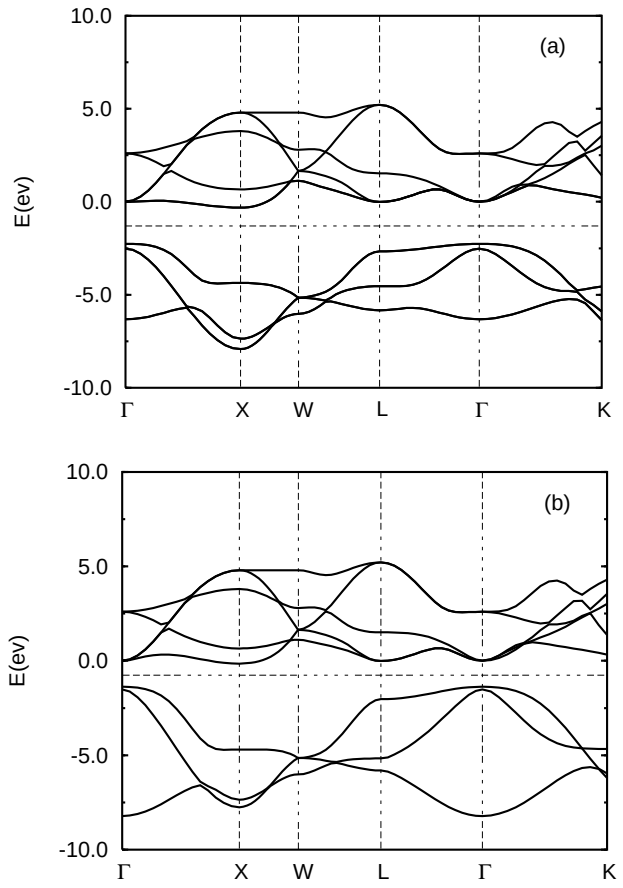

FIG. 10. Band structure of LaH_3 of model Hamiltonian (17) using Gutzwiller approximation. In (a) the crystal field is included in estimating the H-H hopping integrals. In (b) the crystal field effect is not included. The actual result is expected to be between (a) and (b).

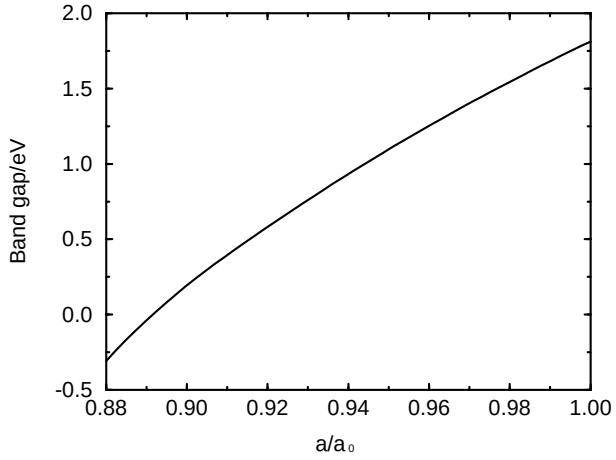

FIG. 11. Band gap of LaH_3 is observed to be a monotonic increasing function of lattice constant a (in unit of a_0). Therefore by exerting large enough pressure on the crystal, the band gap will be closed up and the originally insulating hydride will become conducting. This transition happens when $a \sim 0.89a_0$.

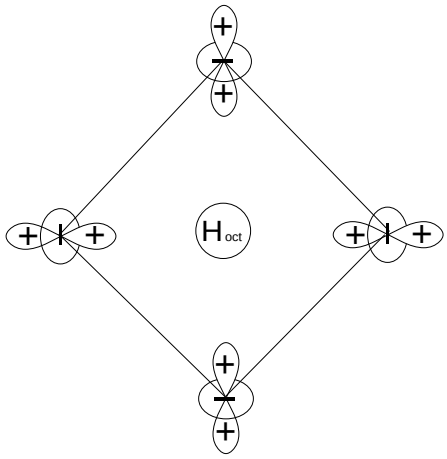

FIG. 12. 2-D illustration of an impurity state. Six neighboring La-5d-e_g orbitals (only 4 of them are shown here) are pointing toward the extra H_{oct}.

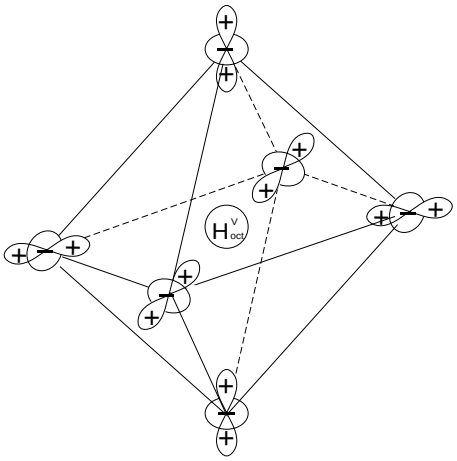

FIG. 13. Diagrammatic illustration of the proposed H_{oct} vacancy state in LaH_3. The center circle represents a H vacancy, forming an n-type impurity center. The surrounding orbits represent phases for the local s-like octahedral La-5d-e_g. The vacancy state has spin-1/2.

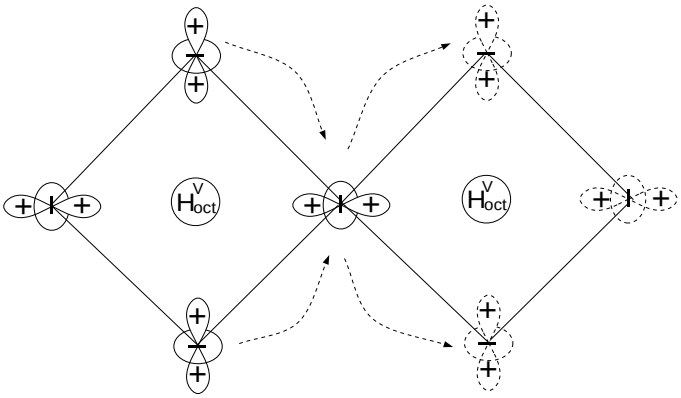

FIG. 14. A 2-D illustration of vacancy state hopping. The dashed line with arrow represents the microscopic hopping process. Note that in 3-D, the nearest neighbor vacancy states have two common La atoms and have a shorter inter-vacancy distance.

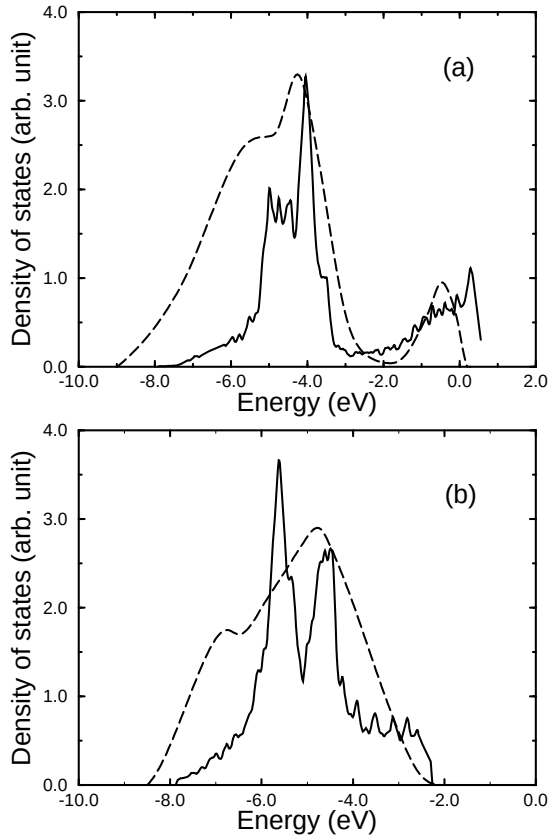

FIG. 15. Density of states for (a) LaH_2 and (b) LaH_3. Solid curves are our calculated results and dashed curves are the experimental data obtained from Peterman *et al.* [36].

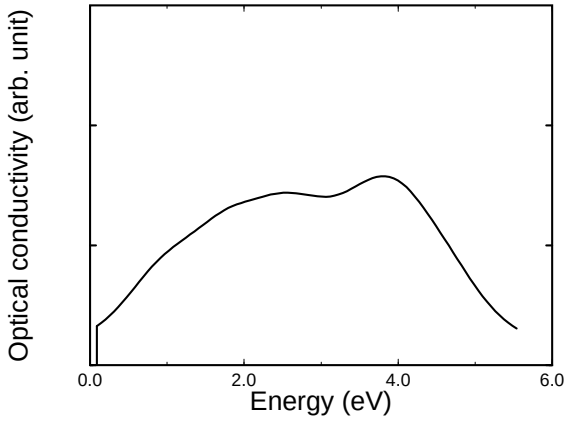

FIG. 16. Optical conductivity due to excitation of electrons from vacancy state to conduction band of LaH_3.